

Electron-impact excitation of the $d^3\Pi_u^-(v = 0, 1, 2, 3; N = 1)$ states of H_2 : Cross sections and anisotropy parameters

G. D. Meneses and L. M. Brescansin

Instituto de Física "Gleb Wataghin," Universidade Estadual de Campinas, 13083-970 Campinas, São Paulo, Brazil

M. T. Lee and S. E. Michelin*

Departamento de Química, Universidade Federal de São Carlos, 13565-905 São Carlos, São Paulo, Brazil

L. E. Machado

Departamento de Física, Universidade Federal de São Carlos, 13565-905 São Carlos, São Paulo, Brazil

G. Csanak

Los Alamos National Laboratory, Los Alamos, New Mexico 87545

(Received 7 September 1994)

We have applied the density-matrix formalism and a distorted-wave approximation scheme to calculate Stokes parameters, polarization fractions, alignment tensors, and orientation vectors for the $d^3\Pi_u^-(v = 0, 1, 2, 3; N = 1)$ states of H_2 , as well as rovibrationally resolved state-to-state differential and integral cross sections for the $X^1\Sigma_g^+(v = 0) \rightarrow d^3\Pi_u^-(v = 0, 1, 2, 3)$ excitation by electron impact at incident energies ranging from 15 to 40 eV. This is a systematic study for H_2 of these quantities as a function of incident energy and final vibrational levels. Good agreement between our calculated Stokes parameters and the only available experimental data is observed. Our results show that these parameters are nearly independent of the vibrational quantum number of the excited state, that the polarization of the radiation emitted by the target in the subsequent decay process increases with increasing incident energies, and that the Stokes parameters are small compared with atomic values even if the fine and hyperfine structure effects are not taken into account.

PACS number(s): 34.80.Gs

I. INTRODUCTION

Considerable experimental and theoretical efforts have been devoted in the past to a better understanding of the dynamics of atomic and (to a much less extent) molecular excitations by electron impact with the help of coherence and correlation parameters (CCP's) [1-4]. The CCP's can be measured in electron-photon coincidence experiments, where the emitted radiation from a specially selected ensemble of atoms or molecules is observed, namely from those atoms or molecules that scatter the electrons into a well defined direction with a well defined energy loss [1,4]. The features of the radiating ensemble of atoms or molecules manifest themselves in the intensity and polarization characteristics of the emitted radiation and quantitatively in the values of the measured Stokes parameters [1-4]. Such an ensemble can in general be characterized by sets of parameters, such as those proposed by Andersen *et al.* [1] and by Fano and Macek [5], that provide physical insight into the result-

ing excited target state. The comparison of the measured CCP's with theory is done at the level of complex excitation amplitudes and their interference rather than at that of the usual excitation cross sections. Thus, while providing more detailed information on the scattering processes, they constitute a most sensitive test of theoretical models and approximations.

The emphasis of coherence and correlation studies has been on the excitation of atoms, mainly on the $^1S_0 \rightarrow ^1,3P_1$ excitations of rare gases, which have been the most thoroughly investigated processes both theoretically and experimentally. In the case of atomic targets, several reviews have summarized the progress in this field over the years [1,6,7]. For molecules, however, although the basic theoretical framework for the interpretation of an electron-photon coincidence experiment was laid down by Blum and Jakubowicz (BJ) in 1978 [8], its application is still very limited since only a few such experiments have so far been reported [9-13]. The main reason for this limitation is that obtaining information as detailed for molecular as for atomic excitations requires the consideration of individual initial, excited, and final rotational states with well defined angular momenta. For these processes, measurements of cross sections and Stokes parameters are still very difficult. McConkey *et al.* [12] have demonstrated, however, the feasibility of an electron-photon coincidence ex-

*Permanent address: Departamento de Física, Universidade Federal de Santa Catarina, Florianópolis, Santa Catarina, Brazil.

periment for a transition involving rotationally resolved states and reported Stokes parameters for the excitation of the $d^3\Pi_u^-(v_1 = 0, N_1 = 1)$ level of H_2 at 25 eV. In addition, rovibrationally resolved relative integral cross sections (ICS's) have been measured by Ottinger and Rox [14] for the excitation of the $c^3\Pi_u^-(v_1 = 0, 1, 2, 3, N_1 = 2)$ levels of H_2 . On the theoretical side, however, in spite of the progress in the analysis of the measured Stokes parameters, until very recently no CCP's had ever been reported for molecules. In a recent Letter [15] we published theoretical distorted-wave results for Stokes parameters and state-to-state rovibrationally resolved (rovibronic) differential cross sections (DCS's) for a molecule. Specifically, we considered the electron-impact excitation of the $d^3\Pi_u^-(v_1 = 0, N_1 = 1)$ level of H_2 from the $X^1\Sigma_g^+(v_0 = 0, N_0 = 1)$ level at the incident energy of $E_0 = 25$ eV, where our theoretical results could be compared with the experimental data of McConkey *et al.* [12]. Since then, the R -matrix calculations of DCS's and CCP's for the transitions $X^3\Sigma_g^-(N_0 = 1) \rightarrow b^1\Sigma_g^+(N_1 = 2, 3)$ and $X^3\Sigma_g^-(N_0 = 1) \rightarrow a^1\Delta_g(N_1 = 2, 3)$ in O_2 were the only to be reported in the literature [16,17].

In the present work we report a calculation of Stokes parameters, alignment tensor, orientation vector, and polarization fractions for the $d^3\Pi_u^-(v_1 = 0, 1, 2, 3; N_1 = 1)$ states of H_2 excited from the $X^1\Sigma_g^+(v_0 = 0, N_0 = 1)$ state by electron impact at incident energies E_0 ranging from 15 to 40 eV, as well as rovibrationally resolved DCS's and ICS's in this energy range. In order to get the rovibrationally resolved state-to-state scattering amplitudes (which are required for the determination of Stokes parameters) we have used the distorted-wave approximation (DWA) combined with the adiabatic-nuclei approximation; for the calculation of the CCP's we have used the density-matrix formalism of BJ. The DWA has been applied successfully in the past to calculate certain DCS's and CCP's for electron-impact excitations of atoms [1,18]. Also, it has been shown that the DWA has given essentially identical cross sections to the Schwinger multichannel method at the two-state level of approximation for excitations leading to the three first excited states of H_2 [19], as well as ICS's that are in good agreement with the experimental data for the $X^1\Sigma_g^+ \rightarrow d^3\Pi_u$ transition [20]. First-order many-body theory (which is equivalent to the particular DWA calculational scheme we have used here [21,19]) has been applied for calculations of CCP's for the 3^3P states of the helium atom and has given results in reasonable agreement with the experimental data [22]. Since the $d^3\Pi_u^-$ state in H_2 is quite atomlike, one can expect that the DWA is suitable as a first theoretical approach for the calculation of CCP's for the excitation of this state. Due to the great difficulty in doing the coincidence experiments, the experimental results are likely to have large error bars. Our purpose is to help experimentalists with the qualitative behavior of the CCP's and their order of magnitude that can be expected.

In Sec. II the method is described in some detail. Some aspects of the calculations are presented in Sec. III, while our results are shown in Sec. IV along with the limited data available for comparison.

II. METHOD

We follow the formulation of BJ, who extended the application of the density-matrix formalism to the interpretation of electron-photon coincidence experiments for molecular targets obeying Hund's case (b) coupling scheme. The applicability of their theory to the transition studied herein was discussed by McConkey *et al.* [12]. Throughout this paper we will follow BJ's definitions and notation: Λ will denote the component of the electronic angular momentum along the molecular axis, S the molecular spin (with component M_S), N the total angular momentum (with component M_N) of the molecule, v the vibrational quantum number, and n all other quantum numbers. The components M_S and M_N are both measured in the laboratory frame. The subscripts 0 and 1 attached to these quantum numbers will refer to the initial and the excited state of the collision process, respectively, and the subscript f will denote the final state after decay. In our case, due to the possibility of various values for M_{N_0} (for which an isotropic distribution is assumed), the initial molecular state will be described by a density operator (or density matrix) of the form

$$\hat{\rho}_0 = \frac{1}{(2N_0 + 1)} \sum_{M_{N_0}} |\Gamma_0\rangle \langle \Gamma_0|. \quad (1)$$

As a result of the partially coherent nature of the initial molecular state, as well as of the unpolarized nature of the incident electron beam, the excited state will also be partially coherent, being described by the density operator

$$\hat{\rho}_1 = \frac{1}{2(2N_0 + 1)} \sum_{M_{N_0}, M_{N_1}, M'_{N_1}, m_{S_0}} f_{\Gamma_1 \Gamma_0} f_{\Gamma_1 \Gamma_0}^* |\Gamma_1\rangle \langle \Gamma_1'|, \quad (2)$$

where m_{S_0} refers to the spin projection of the incident electron, $|\Gamma\rangle = |nv\Lambda SM_S NM_N\rangle$ denotes a molecular state in the uncoupled representation, and $f_{\Gamma_1 \Gamma_0}$ is the electron scattering amplitude for the $\Gamma_0 \rightarrow \Gamma_1$ process. The excited radiating state can, however, be equivalently described by the average values of a set of tensorial operators $T(N_1 N_1')_{KQ}^\dagger$ ($K = 0, 1, 2; -K \leq Q \leq K$) (usually called state multipoles) in that state [8], which, as discussed in our previous work [15], are actually time dependent.

The Stokes parameters are defined in terms of these state multipoles by Eqs. (32a)–(32d) of Ref. [8]. Those equations have been particularized for the experimental geometry [12], resulting in

$$\begin{aligned} \eta_0 = A & \left[\sum_{N_f, N_1, N_1'} W(N_f N_1 N_1') \frac{2(-1)^{N_1 + N_f}}{3(2N_1 + 1)^{1/2}} G_0(t) \right. \\ & \times \left\langle T(N_1' N_1)_{00}^\dagger \right\rangle + \sum_{N_f, N_1, N_1'} W(N_f N_1 N_1') G_2(t) \\ & \times \left\{ \begin{matrix} 1 & 1 & 2 \\ N_1 & N_1' & N_f \end{matrix} \right\} \left(\left\langle T(N_1' N_1)_{22}^\dagger \right\rangle \right. \\ & \left. \left. + \sqrt{\frac{1}{6}} \left\langle T(N_1' N_1)_{20}^\dagger \right\rangle \right) \right], \quad (3) \end{aligned}$$

$$\eta_1 = -\frac{2A}{\eta_0} \sum_{N_f, N_1, N'_1} W(N_f N_1 N'_1) G_2(t) \times \left\{ \begin{matrix} 1 & 1 & 2 \\ N_1 & N'_1 & N_f \end{matrix} \right\} \langle T(N'_1 N_1)^\dagger_{21} \rangle, \quad (4)$$

$$\eta_2 = -\frac{2iA}{\eta_0} \sum_{N_f, N_1, N'_1} W(N_f N_1 N'_1) G_2(t) \times \left\{ \begin{matrix} 1 & 1 & 1 \\ N_1 & N'_1 & N_f \end{matrix} \right\} \langle T(N'_1 N_1)^\dagger_{11} \rangle, \quad (5)$$

$$\eta_3 = \frac{A}{\eta_0} \sum_{N_f, N_1, N'_1} W(N_f N_1 N'_1) G_2(t) \times \left\{ \begin{matrix} 1 & 1 & 2 \\ N_1 & N'_1 & N_f \end{matrix} \right\} \left[-\langle T(N'_1 N_1)^\dagger_{22} \rangle + \sqrt{\frac{3}{2}} \langle T(N'_1 N_1)^\dagger_{20} \rangle \right], \quad (6)$$

where A is a factor containing the dipole matrix elements for the transition $\Gamma_1 \rightarrow \Gamma_f$ involved in the radiative decay process, $W(N_f N_1 N'_1)$ is a geometrical factor defined by BJ [Eq. (32e)], and the coefficients $G(t)_K$ are relaxation factors describing the time dependence of the state multipoles, due to the fine and the hyperfine terms in the Hamiltonian. These coefficients are given by Eq. (21) of BJ. However, as noted by McConkey *et al.* [12], since the resolution time of the photon detector is much longer than the radiative lifetime of the fine and the hyperfine levels, the observed radiation will be influenced only by a time average of those quantities

$$\bar{G}_K = \int_0^\infty G(t)_K dt. \quad (7)$$

For the $X^1\Sigma_g^+(N_0 = 1) \rightarrow d^3\Pi_u^-(N_1 = 1)$ transition in H_2 , these averaged perturbation factors are $\bar{G}_0 = 0.962$, $\bar{G}_1 = 0.375$, $\bar{G}_2 = 0.115$, and $W(N_f N_1 N'_1) = 1.498$ [12]. By inserting these values into Eqs. (4)–(6) and considering $N'_1 = N_f = 1$, we obtain

$$\eta_1 = -0.058 \langle T(11)^\dagger_{21} \rangle / D, \quad (8)$$

$$\eta_2 = -0.188i \langle T(11)^\dagger_{11} \rangle / D, \quad (9)$$

$$\eta_3 = 0.029 [\sqrt{3/2} \langle T(11)^\dagger_{20} \rangle - \langle T(11)^\dagger_{22} \rangle] / D, \quad (10)$$

where $D = 0.555 \langle T(11)^\dagger_{00} \rangle + 0.029 \langle T(11)^\dagger_{22} \rangle + 0.012 \langle T(11)^\dagger_{20} \rangle$.

The averages of the state multipoles in Eqs. (3)–(6) and (8)–(10) are in turn related to the state-to-state scattering amplitudes of the excitation process $f_{N_1 M_{N_1} N_0 M_{N_0}}$ by Eq. (15) of Ref. [8]. In our case, where there is only one total spin channel ($S = \frac{1}{2}$), this equation reduces to

$$f_{N_1 M_{N_1} N_0 M_{N_0}} = \sqrt{2\pi} \sum_{l, l_0, m'} i^{l_0 - l} [(2l_0 + 1)(2N_0 + 1)(2N_1 + 1)]^{1/2} Y_{lm'}(\hat{k}_1) \times \sum_{m, m_0, J} \frac{1}{(2J + 1)} C(l N_1 J; m' M_{N_1}) C(l_0 N_0 J; \Lambda_0 M_{N_0}) C(l_0 N_0 J; m_0 \Lambda_0) \times [\delta_{m + \Lambda_1, m_0 + \Lambda_0} T_{lm, l_0 m_0}^{vv_0} C(l N_1 J; -m - \Lambda_1) + (-1)^{N_1} \delta_{m - \Lambda_1, m_0 + \Lambda_0} T_{lm, l_0 m_0}^{vv_0} C(l N_1 J; -m \Lambda_1)] \delta_{M_{N_1} + m', M_{N_0}}, \quad (16)$$

$$\langle T(11)^\dagger_{KQ} \rangle = \text{Tr}[\hat{\rho}_1 T(11)^\dagger_{KQ}] = \frac{1}{3} \sum_{M_{N_1}, M_{N_1}, M_{N_0}} f_{1 M_{N_1} 1 M_{N_0}} f_{1 M_{N_1} 1 M_{N_0}}^* \times (-1)^{1+K+Q-M_{N_1}} \times (2K + 1)^{1/2} \begin{pmatrix} 1 & 1 & K \\ -M_{N_1} & M_{N_1} & Q \end{pmatrix}. \quad (11)$$

The diagonal elements of $\hat{\rho}_1$ give the state-to-state rovibronic DCS's for the excitation of the M_{N_1} rotational sublevels. In the present case these DCS's can be written as

$$\sigma_{M_{N_1}}(\theta) = \frac{k_1}{6k_0} \sum_{M_{N_0}} |f_{1 M_{N_1} 1 M_{N_0}}(\theta)|^2 \quad (12)$$

and the ICS's as

$$Q_{M_{N_1}} = 2\pi \int_0^\pi \sigma_{M_{N_1}}(\theta) \sin(\theta) d\theta. \quad (13)$$

In the adiabatic-nuclei framework the scattering amplitude can be written in the form [21,23]

$$f_{N_1 M_{N_1} N_0 M_{N_0}} = \langle v_1 \Lambda_1 N_1 M_{N_1} | f_{\text{el}}(\vec{k}_0, \vec{k}_1; \vec{R}) | v_0 \Lambda_0 N_0 M_{N_0} \rangle, \quad (14)$$

where $f_{\text{el}}(\vec{k}_0, \vec{k}_1; \vec{R})$ is the fixed-nuclei electronic scattering amplitude, \vec{k}_0 (\vec{k}_1) is the momentum of the incident (scattered) electron, and $R = |\vec{R}|$ is a given internuclear distance.

In order to obtain the amplitudes $f_{N_1 M_{N_1} N_0 M_{N_0}}$ we have calculated $f_{\text{el}}(\vec{k}_0, \vec{k}_1; \vec{R})$ using the DWA [21,19]. The calculational scheme adopted here, in which both the incident and the scattered electron wave functions are calculated in the static-exchange potential field of the target ground state, makes our DWA scheme equivalent to the first-order many-body theory [24]. This approximation was used in a previous work to calculate the vibrationally resolved DCS's for the excitation $X^1\Sigma_g^+(v_0 = 0) \rightarrow d^3\Pi_u^-(v = 0, 1, 2, 3)$ in H_2 by electron impact [20]. The procedure concerning the vibrational part of Eq. (14) is described in detail in Ref. [20]. For the rotational part we have used the linear combination of symmetric top wave functions appropriate for ortho- H_2 [25–27]:

$$\mathcal{R}_{N, M_N, \Lambda}(\hat{R}) = \left(\frac{2N + 1}{16\pi^2} \right)^{1/2} [\mathcal{D}_{M_N \Lambda}^N(\hat{R}) + (-1)^N \mathcal{D}_{M_N - \Lambda}^N(\hat{R})]. \quad (15)$$

After performing the integrations in Eq. (14) we obtained the following final expression for the scattering amplitudes:

where the $C(l_1 l_2 l_3; m_1 m_2)$ are the usual Clebsch-Gordan coefficients and

$$T_{lm,l_0 m_0}^{vv_0} = \langle v | T_{lm,l_0 m_0}(R) | v_0 \rangle. \quad (17)$$

In Eq. (17), $T_{lm,l_0 m_0}(R)$ are the partial-wave components of the R -dependent electronic transition matrix $\langle k_1 l m, n_1 | T_{e1} | k_0 l_0 m_0, n_0 \rangle$ defined in Eqs. (13) and (14) of Ref. [21].

From Eq. (16) it follows that

$$m + \Lambda_1 = m_0 + \Lambda_0, \quad (18)$$

$$M_{N_1} + m' = M_{N_0}, \quad (19)$$

$$|N_0 - l_0| \leq J \leq N_0 + l_0, \quad (20)$$

$$|N_1 - l| \leq J \leq N_1 + l, \quad (21)$$

where l (l_0) is the scattered (incident) electron angular momentum and m (m_0) its projection on the molecular axis; m' is the projection of l on the z axis in the laboratory frame, which is taken as the exciting beam direction. Equations (20) and (1) express the conservation of the total angular momentum, while Eqs. (18) and (19) represent the conservation of the total angular momentum projection in the body and laboratory frames, respectively. Also, from symmetry considerations, only terms with $l + l_0$ odd need to be included in the partial-wave expansion of $f_{e1}(\vec{k}_0, \vec{k}_1; \vec{R})$.

III. DETAILS OF CALCULATION

The numerical procedure and details of the present DWA calculation are essentially the same as in Ref. [20]. The standard [5s2p] contracted set of Cartesian-Gaussian functions of Huzinaga [28], augmented with one uncontracted s function with exponent 0.03 and four uncontracted p functions with exponents 0.06, 0.023, 0.009, and 0.001 on the hydrogen nuclei, is used for both the self-consistent field (SCF) and the improved virtual orbitals calculations. Using this basis set, the calculated SCF energy is -1.13330 a.u. at the equilibrium geometry ($R_e = 1.4006$ a.u.), compared with the Hartree-Fock limit of -1.13363 a.u. [29]. The calculated vertical excitation energy, at $R = R_e$, was 14.5619 eV, to be compared with the experimental value of 14.3893 eV for the $v_0 = 0 \rightarrow v_1 = 2$ transition [30]. Six symmetries ($\sigma_g, \sigma_u, \pi_g, \pi_u, \delta_g, \delta_u$) were considered in the calculation of both incident and scattered electron wave functions, for each internuclear distance. Experimental excitation energies [30] for each specific vibronic transition [$X^1\Sigma_g^+(v_0 = 0) \rightarrow d^3\Pi_u^-(v_1 = 0, 1, 2, 3)$] were used to compute the energy of the scattered electron. In order to ensure convergence of all angular momentum expansions, terms up to $l_{\max} = 10$ were included for each symmetry. We have calculated the initial and the final continuum wave functions of the scattered electrons using the Schwinger variational iterative method (SVIM) [31]. The initial L^2 basis set used in the SVIM is listed in Ref. [20]. In order to perform the integration in Eq. (14), the vibrational wave functions $|v_0\rangle$ and $|v_1\rangle$ were calcu-

lated using the numerical method of Cooley [32] from the experimental potential curves in a 501-point grid covering the $0.8 \leq R \leq 3.5$ a.u. range. The potential curves given by Spindler [33] and Dieke [30] were used to calculate the vibrational functions of the ground state and for the excited state, respectively. After interpolating the T matrix over the same grid, Simpson's rule was used to evaluate the integral in Eq. (14).

IV. RESULTS AND CONCLUSIONS

A. Stokes parameters, alignment tensor, and orientation vector

Figures 1(a)–1(d) show the calculated Stokes parameters η_1 , η_2 , and η_3 and the degree of polarization P [i.e., the magnitude of the vector (η_1, η_2, η_3)] for the $d^3\Pi_u^-(v_1 = 0, N_1 = 1)$ state of H_2 excited by electron impact at 25 eV, along with the only available experimental data of McConkey *et al.* [12]. In our previous work [15], these data were already analyzed. The calculated polarization correlations were shown to be essentially small and in general agreement with the measured values, within the experimental error. This smallness reflects the fine- and hyperfine-structure relaxation effects, which are known [34] to reduce significantly the angular anisotropy and the polarization of the radiation emitted by the target in the subsequent decay process. Quantitatively, these effects come in through the values of the perturbation factors \bar{G}_K of Eq. (7). It was also noted that, as for the rare gases, the net transfer of angular momentum (the negative of η_2) is positive for small scattering angles. In fact, a remarkable similarity in shape between our η_2 results and the corresponding values for the 3^3P states of helium was observed [22]. This similarity is not surprising due to the atomiclike nature of the $d^3\Pi_u^-$ state of H_2 . The contribution of η_2 to P is dominant (except around 0° and 180°), resulting in two maxima in the degree of polarization curve. Calculated results for the Stokes parameters without taking into account the relaxation effects are also included in Fig. 1. It is interesting to note that even in this case the degree of polarization is substantially smaller than the equivalent values obtained for atoms [1]. This depolarization probably results from averaging over magnetic sublevels of the $N_0 = 1$ states and summing over the $N_f = 1$ states. As expected, the calculated results accounting for the relaxation effects are in better agreement with the experimental data.

Stokes parameters for several energies in the range 15–40 eV were also calculated. For the energies considered, the angular dependence of all Stokes parameters was found to be very similar to those shown in Fig. 1. As an illustration, in Fig. 2 we present the angular dependence of the degree of polarization P for the $v_0 = 0 \rightarrow v_1 = 1$ vibrational channel and for that energy range. The two maxima in the angular dependence seen at 25 eV remain in the entire energy range. The first maximum is shifted towards 90° and its magnitude increases rapidly with the increase of the incident energy.

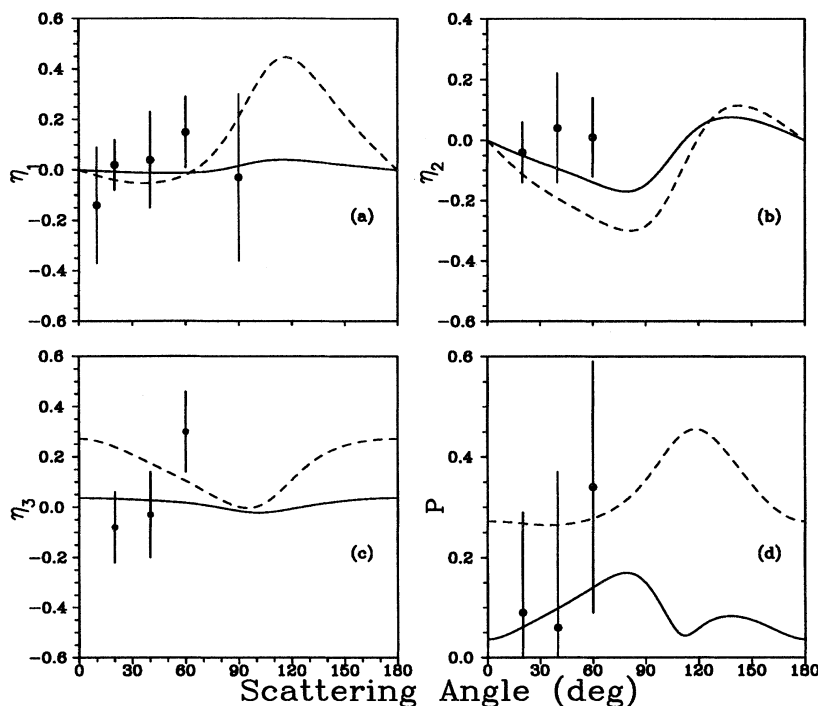


FIG. 1. Stokes parameters (a) η_1 , (b) η_2 , (c) η_3 , and (d) degree of polarization for the state $d^3\Pi_u^-(v_1 = 0, N_1 = 1)$ of H_2 excited by electron impact at 25 eV. Solid line, present results including relaxation effects; dashed line, present results without relaxation effects; dots with error bars, experimental data from Ref. [11].

The calculated value (0.036) of the pseudothreshold polarization (η_3 in the forward direction, which coincides with P , since $\eta_1 = \eta_2 = 0$ in this direction) is independent of the incident energy and is nearly of the same magnitude as that reported previously by McConkey *et al.* (0.025) [12].

In Fig. 3 we show the angular dependence of P for the excited states $d^3\Pi_u^-(v_1 = 0, 1, 2, 3; N_1 = 1)$, at the incident energy $E_0 = 25$ eV. Both the shape and the magnitude of the degree of polarization are almost the same

regardless of the vibrational quantum levels of the excited state. Although not shown here, the same behavior was also observed for η_1 , η_2 , and η_3 in the energy range covered. Particularly, the pseudothreshold polarization was observed to be independent of the vibrational levels of the excited state. In fact, the independence of the pseudothreshold value of the degree of polarization from both the incident energy and the final vibrational quantum numbers is expected, since it can be shown that for the transition studied herein it reduces to a geometrical factor.

The Stokes parameters characterize the polarization of the radiation emitted in the decay process, after the re-

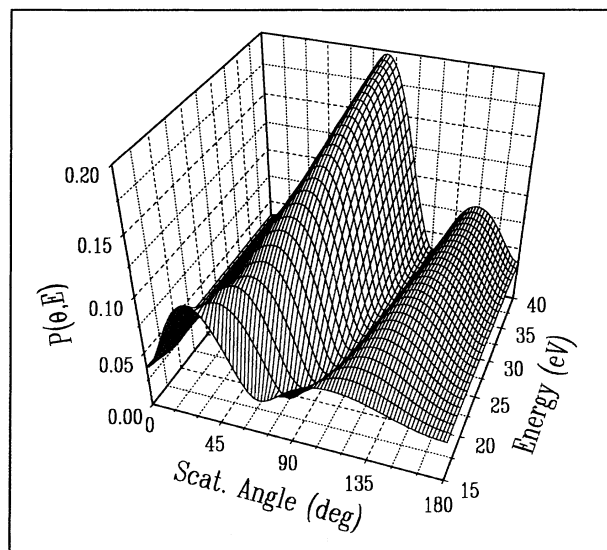


FIG. 2. Degree of polarization P for the excited $d^3\Pi_u^-(v_1 = 1; N_1 = 1)$ state of H_2 .

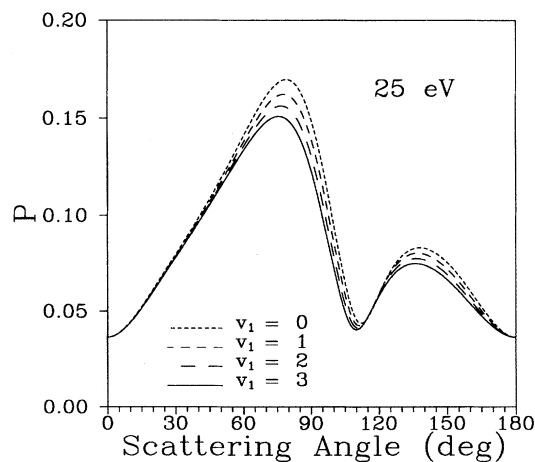


FIG. 3. Degree of polarization P for the excited $d^3\Pi_u^-(v_1 = 0, 1, 2, 3; N_1 = 1)$ states of H_2 for incident energy of 25 eV.

laxation of the electronically excited state takes place. However, several sets of parameters have been proposed [1,5,35] for the description of the excited state immediately after the collision (before relaxation). In this work, Fano's parametrization was chosen, similarly to that used by Nordbeck *et al.* for O_2 [16]. Figure 4(a) shows the orientation vector $\langle T(11)_{11}^\dagger \rangle / \sigma$ and Figs. 4(b)–4(d) show the alignment parameters $\langle T(11)_{20}^\dagger \rangle / \sigma$, $\langle T(11)_{21}^\dagger \rangle / \sigma$, and $\langle T(11)_{22}^\dagger \rangle / \sigma$, respectively, for the $d^3\Pi_u^-(v_1 = 1; N_1 = 1)$ excited state of H_2 as a function of the scattering angle in the incident energy range of 15–40 eV. Although not shown here, the energy and the angular dependence of these parameters for other final vibrational levels ($v_1 = 0, 2, 3$) are very similar to those shown in Fig. 4. Unfortunately, there are neither experimental nor other theoretical results available for this molecule to compare with. However, our calculated values of the alignment tensor and the orientation vector are of comparable magnitude to those obtained by Nordbeck *et al.* for O_2 [16].

B. Cross sections and polarization fractions

In Fig. 5 we present the magnetic-sublevel-specific rovibrationally resolved and total (summed over magnetic sublevels) DCS's for the excitation $X^1\Sigma_g^+(v_0 = 0, N_0 = 1) \rightarrow d^3\Pi_u^-(v_1 = 0, N_1 = 1)$ of H_2 for $E_0 = 20$

eV. Again, there are no experimental data to compare with. An interesting feature is that the forward and the backward DCS's for a magnetic sublevel with $M_{N_1} = 0$ vanish. The same behavior is observed for the $^1S \rightarrow n^1P$ excitations in the helium atom, for example, but for the magnetic sublevel $M_L = 1$ [3]. This can be understood in terms of symmetry considerations [36] and angular momentum conservation laws. For atoms, at $\theta = 0^\circ$ and $\theta = 180^\circ$, Eq. (19) reduces to $M_{L_1} = M_{L_0}$. Therefore, for an atomic $S \rightarrow P$ transition only the magnetic sublevel $M_{L_1} = 0$ can be excited at those angles. For molecules, however, the analysis is more involved. First, at $\theta = 0^\circ$ and $\theta = 180^\circ$, $m' = 0$, thus resulting in $M_{N_1} = M_{N_0}$ in Eq. (19). Second, as Table I of Ref. [36] applies to this case (homonuclear molecule, $\vec{K} = \vec{k}_1 - \vec{k}_0$ parallel to the incident electron direction), molecules rotating in a plane parallel to the exciting beam direction ($M_{N_1} = 0$) cannot contribute to the $X^1\Sigma_g^+ \rightarrow d^3\Pi_u^-$ differential cross sections. Thus, since in our case $N_0 = 1$, this excitation takes place only if the molecule is rotating in a plane perpendicular to the exciting beam direction, that is, if $M_{N_0} = 1$. These arguments have been used in the context of pseudothreshold polarization [37] analysis for H_2 .

In Fig. 6 we show the total (summed over magnetic sublevels) DCS for the excitation $X^1\Sigma_g^+(v_0 = 0; N_0 = 1) \rightarrow d^3\Pi_u^-(v_1 = 1; N_1 = 1)$ of H_2 in the

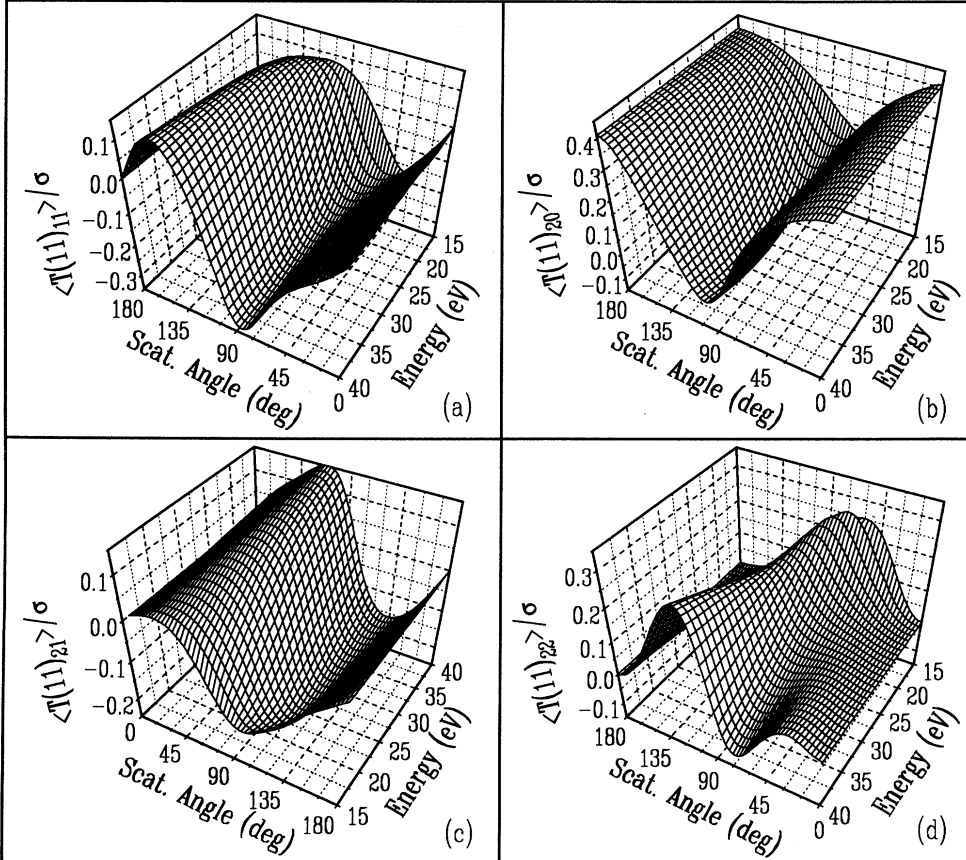


FIG. 4. Orientation vector (a) $\langle T(11)_{11}^\dagger \rangle / \sigma$ and alignment tensors, (b) $\langle T(11)_{20}^\dagger \rangle / \sigma$, (c) $\langle T(11)_{21}^\dagger \rangle / \sigma$, and (d) $\langle T(11)_{22}^\dagger \rangle / \sigma$ for the $X^1\Sigma_g^+(v_0 = 0, N_0 = 1) \rightarrow d^3\Pi_u^-(v_1 = 0, N_1 = 1)$ of H_2 by electron impact at 25 eV.

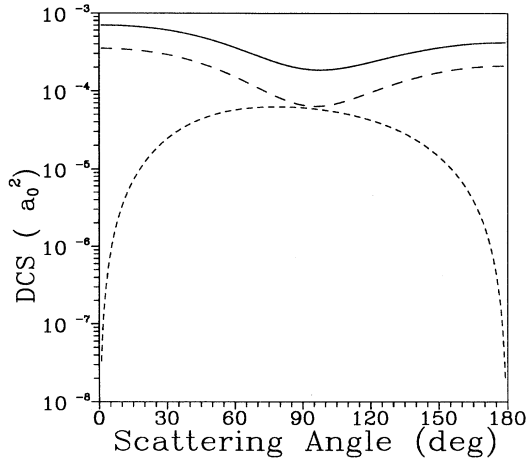


FIG. 5. Rovibrationally resolved DCS's for the excitation $X^1\Sigma_g^+(v_0 = 0, N_0 = 1) \rightarrow d^3\Pi_u^-(v_1 = 0, N_1 = 1)$ of H_2 by electron impact at 20 eV. Long-dashed line, present results for the magnetic sublevel $M_{N_1} = 1$; short-dashed line, present results for the magnetic sublevel $M_{N_1} = 0$; solid line, present results for the total (summed over magnetic sublevel) DCS's.

energy range 15–40 eV. At the low-energy limit (15 eV) the DCS's are essentially backward enhanced, but at the high-energy limit (40 eV), the DCS's become forward enhanced, reflecting the contribution of higher partial waves to the cross sections. Although not shown, the curves for other final $v_1 = 0, 2, 3$ are essentially similar.

Figure 7 shows our calculated vibrationally resolved ICS's for the $v_0 = 0 \rightarrow v_1 = 0, 1, 2, 3$ transitions. The maxima are slightly shifted to higher energies with the increase of the final vibrational quantum number. In addition, for $E_0 \geq 25$ eV, all four curves are nearly parallel,

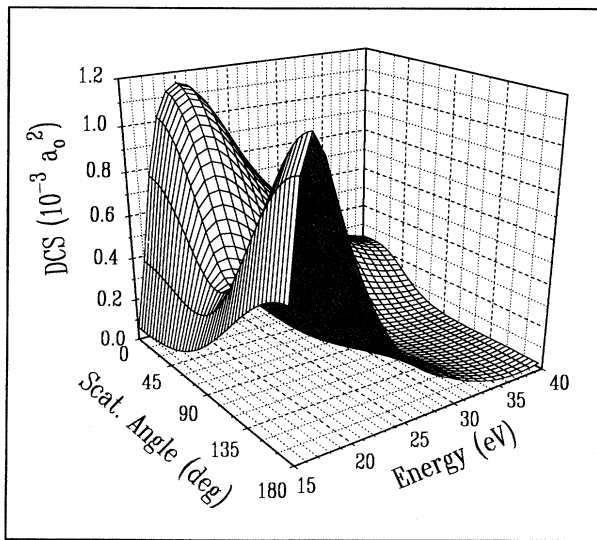


FIG. 6. Total (summed over magnetic sublevels) DCS's for the excitation $X^1\Sigma_g^+(v_0 = 0, N_0 = 1) \rightarrow d^3\Pi_u^-(v_1 = 1, N_1 = 1)$ of H_2 .

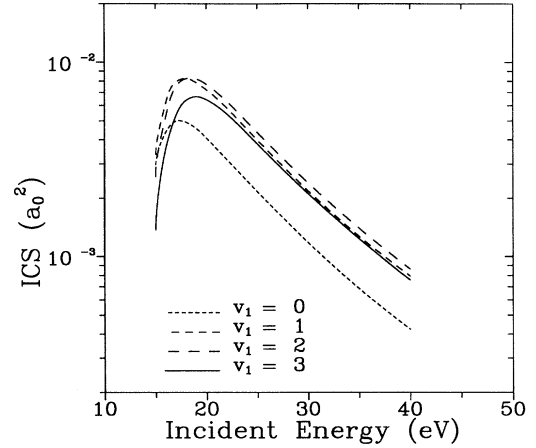


FIG. 7. Vibrationally resolved ICS's for the $X^1\Sigma_g^+(v_0 = 0, N_0 = 1) \rightarrow d^3\Pi_u^-(v_1 = 0, 1, 2, 3; N_1 = 1)$ transitions of H_2 .

reflecting the validity of the Franck-Condon approximation in this energy region [20].

In the case of the axially symmetric process when the emitted radiation is detected but the scattered electron is not, experimentalists usually measure the linear polarization fraction

$$\mathcal{P} = \frac{I(0^\circ) - I(90^\circ)}{I(0^\circ) + I(90^\circ)}, \quad (22)$$

where $I(\alpha)$ denotes the intensity of light transmitted through a polarimeter oriented at the angle α measured with respect to the incident beam axis and the light is observed in a direction perpendicular to it. This polarization fraction can also be expressed in terms of the integrated magnetic sublevel cross sections $Q_{M_{N_1}}$ [8,38]. For our particular case the relation is

$$\mathcal{P} = \frac{3\bar{G}_2(Q_1 - Q_0)}{Q_0(4\bar{G}_0 - \bar{G}_2) + Q_1(8\bar{G}_0 + \bar{G}_2)}. \quad (23)$$

This polarization fraction, both when the coupling of the fine- and hyperfine-structure levels is considered and when this coupling is neglected, is shown in Fig. 8 as a function of the incident energy. It is observed, as was the case for the Stokes parameters, that the hyperfine-structure relaxation effects also reduce significantly the magnitude of the polarization fraction. From Eq. (23) it follows that \mathcal{P} is bounded according to the relations: $-1.0 \leq \mathcal{P} \leq 0.33$ (without relaxation) and $-0.092 \leq \mathcal{P} \leq 0.044$ (with relaxation). These upper and lower limits were obtained taking $Q_1 = 0$ and $Q_0 = 0$, respectively, and using the corresponding perturbation coefficients \bar{G}_0 and \bar{G}_2 given above. Our calculated Stokes parameters converge to the upper limits at the inelastic threshold energy (where $Q_1 = 0$) for both (with and without relaxation) cases. Nevertheless, in the energy range studied herein, no evidence has been found that the polarization fractions would converge to the lower limits. This analysis is consistent with the results of the

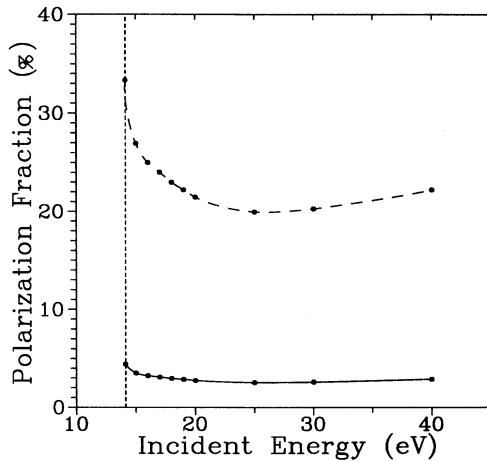


FIG. 8. Polarization fraction for the $X^1\Sigma_g^+$ ($v_0 = 0, N_0 = 1$) \rightarrow $d^3\Pi_u^-$ ($v_1 = 1, N_1 = 1$) transition of H_2 as a function of the incident energy. Solid line: present results including relaxation effects; dashed line: present results without relaxation effects.

magnetic-sublevel-specific ICS's (Q_1 and the Q_0) shown in Fig. 9. Actually, no crossing is observed between the Q_1 and the Q_0 curves in this energy range. This crossing, however, might happen for higher energies, thus leading to a negative lower limit for \mathcal{P} , as suggested by Hammond *et al.* in their study of electron-helium scattering [39].

In summary, we have applied the density-matrix formalism and the DWA to calculate Stokes parameters, alignment tensor, orientation vector, and polarization fraction for the $d^3\Pi_u^-(v_1 = 0, 1, 2, 3; N_1 = 1)$ in H_2 , as well as state-to-state rovibrationally resolved DCS's and ICS's for the excitation $X^1\Sigma_g^+(v_0 = 0; N_0 = 1) \rightarrow d^3\Pi_u^-(v_1 = 0, 1, 2, 3; N_1 = 1)$. The smallness of our calculated polarization correlations reinforces the pioneering experimental findings of McConkey *et al.* [12]. Unfortunately, there are not yet enough experimental results that could help for a more consistent analysis. This is a systematic study of such parameters for molecules as a func-

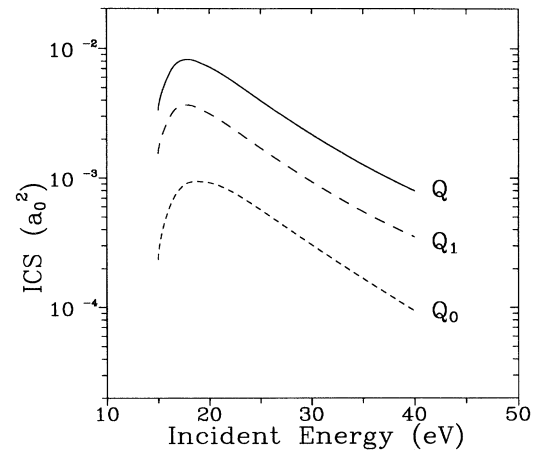


FIG. 9. Magnetic-sublevel-specific (Q_0 and Q_1) and summed (Q) integral cross sections for the $X^1\Sigma_g^+$ ($v_0 = 0, N_0 = 1$) \rightarrow $d^3\Pi_u^-$ ($v_1 = 1, N_1 = 1$) transition of H_2 .

tion of the incident energy and final vibrational quantum states. The nearly independent character of these parameters from the final vibrational quantum states has been verified. Considering the scarcity and the inaccuracy of the experimental data, it is hoped that our work will stimulate further developments in coincidence experiments and then serve as a comparison with the results obtained.

ACKNOWLEDGMENTS

This work was partially supported by the Brazilian agencies CNPq, FAPESP, and FINEP-PADCT. S.E.M. acknowledges CAPES-PICD for financial support. The authors thank Dr. S. Trajmar and Dr. D. C. Cartwright for helpful discussions. One of us (G.C.) wants to acknowledge the financial support from the U.S. Department of Energy and from the NSF (OIP).

-
- [1] N. Andersen, J. W. Gallager, and I. V. Hertel, *Phys. Rep.* **165**, 1 (1988).
 - [2] K. Becker, A. Crowe, and J. W. McConkey, *J. Phys. B* **25**, 3885 (1992).
 - [3] G. Csanak, D. C. Cartwright, and S. Trajmar, *Phys. Rev. A* **45**, 1625 (1992).
 - [4] J. Slevin and S. Chwirot, *J. Phys. B* **23**, 165 (1990).
 - [5] U. Fano and J. Macek, *Rev. Mod. Phys.* **45**, 553 (1973).
 - [6] J. Slevin, *Rep. Prog. Phys.* **47**, 461 (1984).
 - [7] K. Blum and H. Kleinpoppen, *Phys. Rep.* **52**, 203 (1979).
 - [8] K. Blum and H. Jakubowicz, *J. Phys. B* **11**, 909 (1978).
 - [9] I. C. Malcolm and J. W. McConkey, *J. Phys. B* **12**, L67 (1979).
 - [10] K. Becker, H. W. Dassen, and J. W. McConkey, *J. Phys. B* **16**, L177 (1983).
 - [11] K. Becker, H. W. Dassen, and J. W. McConkey, *J. Phys. B* **17**, 2535 (1984).
 - [12] J. C. McConkey, S. Trajmar, J. C. Nickel, and G. Csanak, *J. Phys. B* **19**, 2377 (1986).
 - [13] M. A. Khakoo and J. W. McConkey, *J. Phys. B* **20**, L175 (1987).
 - [14] Ch. Ottinger and T. Rox, *Phys. Lett. A* **161**, 135 (1991).
 - [15] G. D. Meneses, L. M. Brescansin, M. T. Lee, S. E. Michelin, L. E. Machado, and G. Csanak, *Phys. Rev. Lett.* **71**, 1701 (1993).
 - [16] R. P. Nordbeck, K. Blum, C. J. Noble, and P. G. Burke, *J. Phys. B* **26**, 3611 (1993).
 - [17] A. Dellen, R. P. Nordbeck, and K. Blum, *Z. Phys. D* **30**, 169 (1994).
 - [18] K. Bartschat and D. H. Madison, *J. Phys. B* **20**, 5839

- (1987), and references therein.
- [19] M. T. Lee, L. M. Brescansin, and M. A. Lima, *J. Phys. B* **23**, 3859 (1990).
- [20] M. T. Lee, L. E. Machado, L. M. Brescansin, and G. D. Meneses, *J. Phys. B* **24**, 509 (1991).
- [21] A. W. Fliflet and V. McKoy, *Phys. Rev. A* **21**, 1863 (1980).
- [22] D. C. Cartwright and G. Csanak, *J. Phys. B* **19**, L485 (1986).
- [23] N. F. Lane, *Rev. Mod. Phys.* **52**, 29 (1980).
- [24] G. Csanak, H. S. Taylor, and R. Yaris, *Phys. Rev. A* **3**, 1322 (1971).
- [25] T. A. Miller and R. S. Freund, *J. Chem. Phys.* **58**, 2345 (1973).
- [26] A. S. Davydov, *Quantum Mechanics* (Pergamon, Oxford, 1965).
- [27] P. L. Rubin, *Opt. Spektrosk.* **20**, 576 (1966) [*Opt. Spectrosc. (USSR)* **20**, 325 (1966)].
- [28] S. Huzinaga, *J. Chem. Phys.* **42**, 1293 (1965).
- [29] W. Kolos and C. C. J. Roothaan, *Rev. Mod. Phys.* **32**, 219 (1960).
- [30] G. H. Dieke, *J. Mol. Spectrosc.* **2**, 494 (1958).
- [31] R. R. Luchese, G. Raseev, and V. McKoy, *Phys. Rev. A* **25**, 2572 (1982).
- [32] J. W. Cooley, *Math. Comput.* **15**, 363 (1961).
- [33] R. J. Spindler, *J. Quant. Spectrosc. Radiat. Transfer* **9**, 597 (1969).
- [34] K. Blum, *Density Matrix Theory and Applications* (Plenum, New York, 1981).
- [35] F. J. da Paixao, N. T. Padial, and G. Csanak, *Phys. Rev. A* **30**, 1697 (1984).
- [36] G. H. Dunn, *Phys. Rev. Lett.* **8**, 62 (1962).
- [37] J. C. McConkey and I. C. Malcolm, *Coherence and Correlation in Atomic Collisions* (Plenum, New York, 1980).
- [38] D. R. Flower and M. J. Seaton, *Proc. Phys. Soc. London* **91**, 59 (1967).
- [39] P. Hammond, W. Karras, A. G. McConkey and J. W. McConkey, *Phys. Rev. A* **40**, 1804 (1989).